Heat Mass Transfer (2012) 48:735–748
DOI 10.1007/s00231-011-0926-1

ORIGINAL

Flow structure, heat transfer and pressure drop in varying aspect ratio two-pass rectangular smooth channels

Waseem Siddique · Lamyaa El-Gabry · Igor V. Shevchuk · Narmin B. Hushmandi · Torsten H. Fransson

Received: 7 March 2011 / Accepted: 9 October 2011 / Published online: 22 October 2011

Abstract Two-pass channels are used for internal cooling in a number of engineering systems e.g., gas turbines. Fluid travelling through the curved path, experiences pressure and centrifugal forces, that result in pressure driven secondary motion. This motion helps in moving the cold high momentum fluid from the channel core to the side walls and plays a significant role in the heat transfer in the channel bend and outlet pass. The present study investigates using Computational Fluid Dynamics (CFD), the flow structure, heat transfer enhancement and pressure drop in a smooth channel with varying aspect ratio channel at different divider-to-tip wall distances. Numerical simulations are performed in two-pass smooth channel with aspect ratio $W_{in}/H = 1{:}3$ at inlet pass and $W_{out}/H = 1{:}1$ at outlet pass for a variety of divider-to-tip wall distances. The results show that with a decrease in aspect ratio of inlet pass of the channel, pressure loss decreases. The divider-to-tip wall distance (W_{el}) not only influences the pressure drop, but also the heat transfer enhancement at the bend and outlet pass. With an increase in the divider-to-tip wall distance, the areas of enhanced heat transfer shifts from side walls of outlet pass towards the inlet pass. To compromise between heat transfer and pressure drop in the channel, $W_{el}/H = 0.88$ is found to be optimum for the channel under study.

W. Siddique (✉) · N. B. Hushmandi · T. H. Fransson
Department of Energy Technology, Royal Institute of Technology (KTH), 100 44 Stockholm, Sweden
e-mail: Waseem.Siddique@energy.kth.se

W. Siddique
Department of Mechanical Engineering, Pakistan Institute of Engineering and Applied Sciences (PIEAS), Islamabad, Pakistan

L. El-Gabry
Department of Mechanical Engineering, American University in Cairo (AUC), Cairo, Egypt

I. V. Shevchuk
MBtech Group GmbH & Co. KGaA, Salierstr. 38, 70736 Fellbach-Schmiden, Germany

List of symbols

C	Specific heat, [J/kg K]
D	Diameter, [mm]
f	Friction factor, $(2\Delta p D_h/\rho U^2 L)$
h	Heat transfer coefficient, [W/(m^2 K)]
H	Height of channel, [mm]
k	Thermal conductivity of the fluid, [W/(m K)]
L	Length of the channel from the inlet to the outlet, [mm]
Nu	Nusselt number, $(h D_h/k)$
p	Pressure, [N/m^2]
Pr	Prandtl number, $(C_p\mu/k)$
Re	Reynolds number, $(\rho U_{in} D_h/\mu)$
T	Temperature, [K]
U	Velocity, [m/s]
W	Width, [mm]

Greek symbols

Δ	Difference
ρ	Density, [kg/m^3]
μ	Viscosity, [kg/s.m]

Subscripts

avg	Average
el	Divider-to-tip wall
in	Inlet
l	Kays et al.
out	Outlet
o	Dittus-Boelter equation

pe Petukhov et al.
st Straight channel
web Divider wall

1 Introduction

The gas turbine industry is always seeking to increase the thermal efficiency of the gas turbine. One way is to increase the turbine inlet temperature. Increasing the operating temperature however leads to some major challenges with the design operating temperature in a gas turbine surpasses the melting temperature of most materials gas turbine blades are made of. For example a common material to make gas turbine blades is Nickel based alloys where gas turbines running temperature (1,350°C) is often more than the melting point of these Nickel based alloys (1,200–1,315°C). Therefore, various techniques have been developed to cool the blades, such as film cooling, impingement cooling and internal passage cooling where coolant from the compressor is fed into passages cast within the turbine blade providing forced convection heat transfer.

Two-pass rectangular channels with 180° bend are used as cooling configurations in internal cooling of the gas turbine blades. Impingement, recirculation and flow separation is characterized by the flow in these two-pass channels. In the bend, regions of varying heat transfer and large pressure losses are present which leads to high thermal gradients and reduction in efficiency [1]. An efficient design of these passages requires obtaining effective overall cooling of the components for the least pressure drop. Over the years the researchers [2–5] have investigated heat transfer and pressure drop in a two-pass smooth channel. Also, while investigating heat transfer and pressure drop in channels with different heat transfer enhancement techniques, smooth channel data has been used as baseline by researchers [6–9]. Studies by Schabacker et al. [10], Liou et al. [11], Chen et al. [12], Son et al. [13] and Elfert et al. [14] have focused attention on the two-pass channels to study flow, pressure distribution and heat transfer characteristics. These studied the flow field in a two-pass smooth channels and provides good information about the flow characters, such as secondary flow, impingement, separation and recirculation induced by turn. It was found that the sharp turn enhances the heat transfer but with large friction losses. The effect of sharp turning flows in a two-pass square channel with smooth walls using the naphthalene mass transfer technique was reported by Park et al. [15]. They found very large spanwise variation in mass (heat) transfer at the turn and upstream of the outlet pass. Han et al. [16] studied the local mass/heat transfer distribution in two-pass square channels with smooth and 90° ribbed walls. It was found that the mass transfer in and after the turn was more than before the turn. This enhancement was attributed to the secondary flow generated by the centrifugal force at the turn.

Wang et al. [17] numerically investigated the effects of secondary flow on heat transfer along the channel with three different turn configurations. These includes, the straight-corner turn, rounded-corner turn and the circular turn. At the turn region, an increase of approximately 30% in the heat transfer was found in case of rounded-corner channel compared to the straight-corner turn. Liou et al. [18] showed that the augmentation of the heat transfer after the turn region is due to the unsteadiness of separation bubbles downstream of the sharp turn. Etemad and Sundén [19] numerically investigated turbulent heat transfer in a rectangular-sectioned 90° bend with an aspect ratio of 6. They found that both standard and low Reynolds k-ε models performed well in predicting the flow in such geometry. They mentioned that the boundary-layer thickness and the flow upstream of the bend are crucial for characterizing the secondary flow, velocity profile, turbulence level and heat transfer in the bend. Salameh et al. [20] measured heat transfer and pressure drop at the bend surface of a U-duct at different Reynolds number and found that heat transfer enhancement at bend is higher at low Reynolds numbers.

Han [21] investigated the effect of channel aspect ratio on heat transfer for five different channel aspect ratios (W/H = 1:4, 1:2, 1:1, 2:1 and 4:1). It was found that for narrow channels, local heat transfer is higher than the wide aspect ratio channel. Han and Park [22] found that a square channel provides better heat transfer than a channel with width more than height. Park et al. [23] showed that pressure drop is affected by the aspect ratio of the channel. It was found that the pressure drop increased between 2 and 18 times as the aspect ratio of the channel changed from narrow (W/H = 1:4) to wide (W/H = 4:1). Astarita and Cardone [24] used Infra Red (IR) thermography technique to investigate the effect of aspect ratio on heat transfer characteristics in sharp-turn channels. Local Nusselt numbers were measured over the bottom wall for small aspect ratio channels (W/H = 5–1). They concluded that the local Nusselt numbers are influenced by variation in aspect ratio. Cai et al. [25] studied the influence of channel aspect ratio on heat transfer characteristics in sharp turn with inclined divider wall. Four different channels with aspect ratio W/H = 8, 4, 2 and 1 were used for the study where the divider wall's inclination was varied from −6° to +6°. They found that for parallel and divergent channels, aspect ratio influences heat transfer characteristics primarily in and after the turn whereas for the convergent channels, the influence of aspect ratio was significant in the entire channel. Pape et al. [1] studied the influence of 180° bends

in a rectangular channel of aspect ratio W/H = 1:4 experimentally using transient liquid crystal thermography and numerically for different Reynolds numbers. They found that the pressure drop increases with varying the tip distance about a relative tip distance of 1.25. They concluded that the tip distance also has an influence on the heat transfer. Below the relative tip distance of 0.75, it increases compared to the case where relative tip distance was 1. A numerical study by Siddique et al. [26] has been performed to study the heat transfer and pressure drop in a two-pass trapezoidal channel with and without ribs. Due to the trapezoidal cross section, the inlet pass aspect ratio was different from the outlet pass.

The present study focus on the CFD simulation of the flow field and heat transfer in two-pass channels connected with 180° bend. The outlet channel has a fixed aspect ratio of 1:1, while the inlet channel has aspect ratio of W_{in}/H = 1:3. The choice of the cross section of the channel and its aspect ratio depends on the location of the channel in chord wise direction of the blade. A channel with rectangular cross section and aspect ratio 1:2 is located in mid chord of the blade. The objectives of the study are to present the flow and thermal fields in two-pass smooth channels and to analyze the effect of changing the aspect ratio of the channel's inlet pass from W_{in}/H = 1:2 to 1:3 on heat transfer and pressure drop. The channel with inlet aspect ratio of 1:3 has height same as a channel with inlet aspect ratio of 1:2, making the width of the channel small in narrow aspect ratio channel. This thus allows more number of channels to fit in the turbine blade. This choice of the aspect ratio has never been studied before thus making this work unique. Also, for a straight channel, heat transfer increases with increase in hydraulic diameter. This study aims on the effect of this increase on the two-pass channel. In addition to that, the purpose of the study is to analyze the effect of changing the divider-to-tip wall distance (W_{el}) on pressure losses and surface heat transfer.

2 Description of the physical models

A schematic of the geometrical model of the smooth two-pass channel used in the study is shown in Fig. 1. Due to symmetry, only half of the channel is simulated.

The inlet pass has aspect ratio ($AR_{in} = W_{in}/H$) of 1:3, while the outlet pass is a square channel i.e., ($AR_{out} = W_{out}/H$) of 1:1. These two are connected by180° bend. The channel height H = 150 mm, while the inlet width W_{in} = 50 mm. The hydraulic diameter of the inlet pass is 75 mm. A divider wall of thickness W_{web} = 20 mm separates the two passes. The edge of this wall has been rounded in the bend region with a curvature radius of 10 mm. The divider-to-tip wall distance (W_{el}) was varied from 50 mm to 150 mm in order to study its effect on the flow and heat transfer.

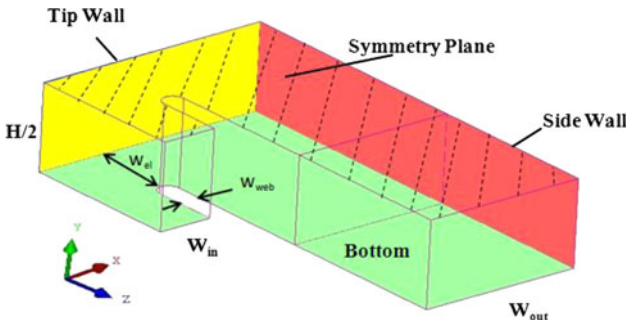

Fig. 1 Schematic view of the smooth two-pass channel with W_{in}/H = 1:3 at inlet pass and W_{out}/H = 1:1 at outlet pass

3 Computational details

3.1 Overview

ANSYS ICEM CFD was used to create geometries as well as to generate the structured mesh. ANSYS FLUENT was used to solve the numerical problem. This code uses the finite volume method to solve the governing equation describing the fluid flow and heat transfer under given boundary conditions. The realizable k–ε turbulence model with enhanced wall treatment was applied for turbulence modeling. Enhanced wall treatment is a method to model the near wall region that combines a two-layer model with enhanced wall functions [27]. Shevchuk et al. [28] has shown that this model performs well for separating flows behind an inclined rib at Reynolds number of 100,000. When enhanced wall treatment is employed, y+ near 1 should be used but a value <4–5 is also acceptable [27]. The near wall regions were meshed, such that the y+ value remains in the range of 1–3 for all cases which is requirement of the near wall treatment used. The residuals for continuity equation were allowed to reach 10^{-6} and that for energy equation to 10^{-9}, in order to assume the solution as converged.

3.2 Defining heat transfer parameters

Jenkins et al. [29] performed experiments to study the effect of divider wall-to- tip wall distance on heat transfer in a two-pass channel. The experiments provide test validation for the current numerical study. In order to compare with the experimental results, the heat transfer definitions and post process follows a similar procedure to the data reduction adopted in experiments. Jenkins et al. [29] used the local bulk temperature profile at discretized axial locations to calculate the local heat transfer coefficients. Shevchuk et al. [28] used CFD to numerically simulate

these experimental results. To calculate heat transfer coefficients, Shevchuk et al. [28] divided the two-pass smooth channel in three regions (inlet pass, bend and outlet pass) and used the volume averaged temperature of each region as reference temperature. To validate this method of calculating Nusselt numbers as equivalent to the method used in experiment, a small comparison has been carried out in the present study. The channel was divided into three regions as done by Shevchuk et al. [28]. In each region, planes were selected at equal distances which were orthogonal to the flow. The area average temperature of each plane was used to calculate Nusselt numbers at the center of the bottom wall of each region. It was compared with the Nusselt numbers based on volume average temperature of each region and also with the temperatures at center of the planes selected. Figure 2, shows the comparison of the three approaches to define Nusselt number for the three regions (inlet pass, bend and outlet pass). At the inlet and outlet pass, the method used by Shevchuk et al. [28] to calculate Nusselt numbers gives results identical to the experimental method of calculating Nusselt numbers with a maximum difference of about 5%. However, in bend region this difference was as high as 13%. Using center line temperature as reference to calculate Nusselt number is only applicable when flow is fully mixed. That condition is attained at outlet pass when fluid is mixed after passing through the bend while at inlet pass it clearly shows incapability to represent actual reference temperature. So the method to use volume averaged temperature, in different regions, as reference to calculate Nusselt number, is adopted in further calculations.

Three different correlations have been used to normalize the Nusselt number in the current study. These are used to compute the Nusselt number for fully developed turbulent flows in smooth circular tubes. The first is the Dittus-Boelter correlation [30] which is used for Reynolds numbers >10,000 and is defined as

$$Nu_o = 0.023 Re^{0.8} Pr^{0.4} \quad (1)$$

The second is a correlation proposed by Kay et al. [31], defined as

$$Nu_l = 0.021 Re^{0.8} Pr^{0.5} \quad (2)$$

The third is a correlation proposed by Petukhov et al. [32], defined as

$$Nu_{pe} = \frac{(f/8) Re\, Pr}{1.07 + 12.7 (f/8)^{0.5} \left(Pr^{2/3} - 1 \right)}, \quad (3)$$

Where

$$f = (1.82 \log_{10} Re - 1.64)^{-2} \quad (4)$$

All the three correlations have been used to normalize the Nusselt number for a periodic segment. Though Dittus-Boelter's correlation is generally used for normalizing therefore, this is used for normalizing other results.

3.3 Grid independence

A detailed grid independence study was carried out where three progressively finer grids were compared, for a fixed geometry with W_{el} of 75 mm ($W_{el}/W_{in} = 1.5$). The three cases namely case 1, case 2 and case 3 comprise of grid sizes equal to 950 K, 1.7 M and 2.6 M cells respectively. Figure 3 shows the bend region of the three meshes. The near wall mesh needed for modeling the viscous sublayer was kept constant so that y+ at the wall is maintained ~ 1 and the growth from the wall is at a ratio of 1.2.

The averaged Nusselt number at the bottom face of the inlet, bend and outlet regions were compared. Figure 4 shows the comparison for the three cases. The area averaged Nusselt number in each region of the channel has been normalized with the Nusselt number ($Nu_{st,avg}$) obtained from a smooth periodic segment. All three cases produced similar results with the maximum deviation of 0.88%. Keeping in mind that the acceptable results should be obtained in a computationally economical way, case 1 was chosen for the further simulations.

3.4 Boundary conditions

At the inlet to the channel, the flow conditions are assumed to be fully developed. In order to apply a fully developed flow boundary condition, at the inlet of the two-pass channel, velocity, temperature and turbulence profiles were mapped from the outlet of a periodic segment to the inlet of the two-pass channel. This periodic segment ensures that the flow is fully developed. The inlet mass flow-rate for the periodic segment corresponds to the Reynolds number of 100,000, with the inlet temperature of 310 K. All walls were kept at a constant temperature of 350 K. Symmetry was introduced at the top of the computational domain, which reduces the computational effort. Ambient conditions were set at the outlet.

The flow is considered incompressible, three dimensional, turbulent and steady with constant thermophysical properties. The simulations have been done for the Prandtl number = 0.72. The working fluid is dry air.

3.5 Validation

Computational Fluid Dynamics (CFD) has shown to be adequate for predicting the heat transfer trends in channels. Over the years extensive work has been done in its development and improvements in its ability to predict. But still, comparisons between numerical simulations and experiments shows differences, which can be due to

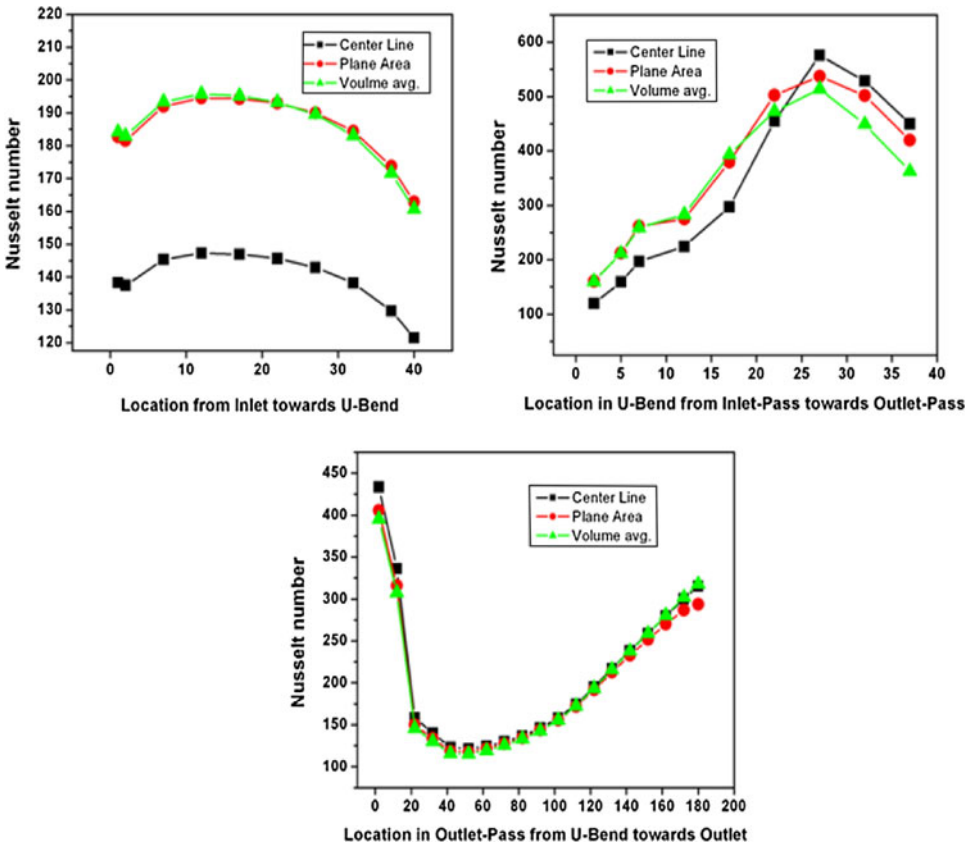

Fig. 2 Comparison of three different methods to calculate Nusselt numbers in three different regions of the channel

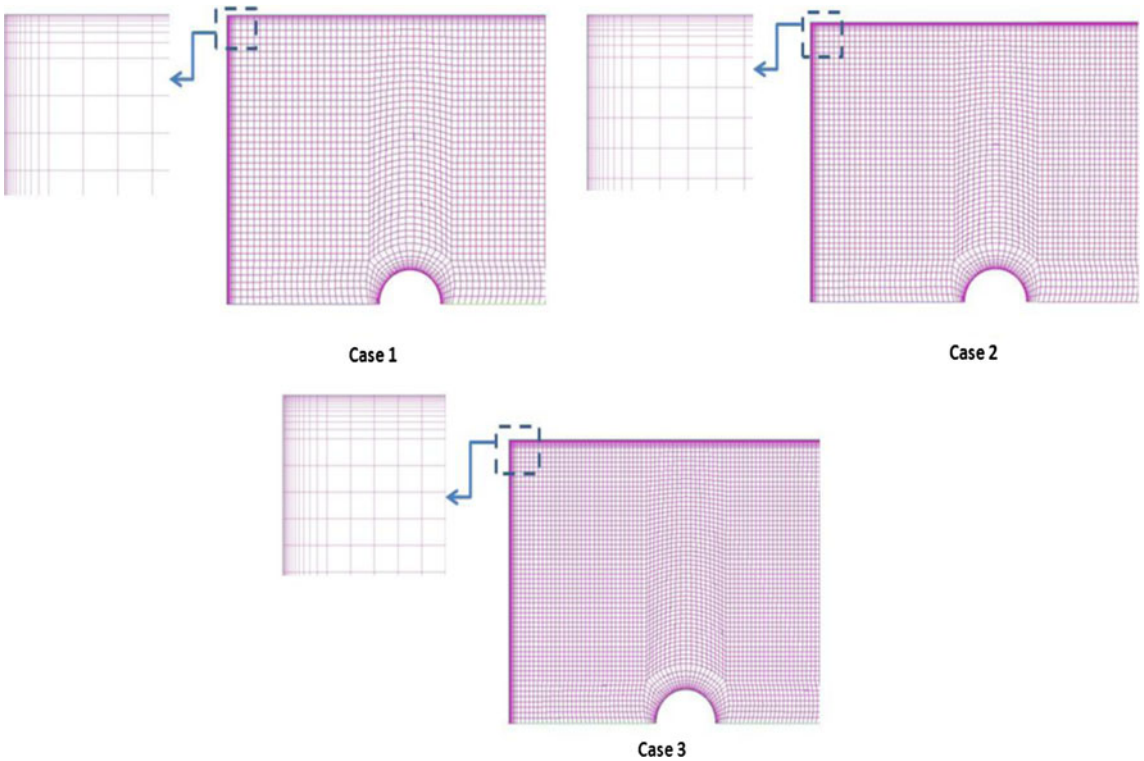

Fig. 3 Three grids at bend section of the channel with $W_{el}/W_{in} = 1.5$

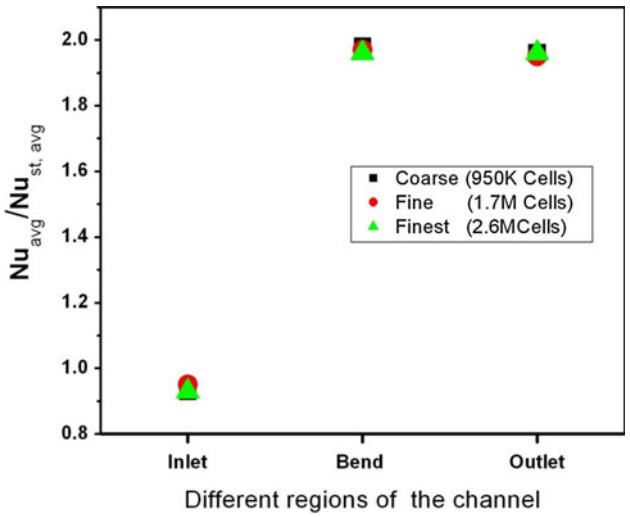

Fig. 4 Comparison of the average Nusselt numbers in different regions for the three cases of the smooth two-pass channel with $W_{el}/W_{in} = 1.5$

inadequate numerical modeling or measurement errors in the experiments. A turbulence model may be very good in predicting the desired results for one case, but might fail in doing so in another case. In practice today, the CFD results for a certain case are compared to experimental results and then, if found good, the numerical results of other similar cases are considered as accepted.

Jenkins et al. [29] performed experiments at Reynolds number = 100,000 to study the effect of tip wall distance on heat transfer for a varying aspect ratio two-pass channel which includes a $W_{in}/H = 1{:}2$ inlet and $W_{out}/H = 1{:}1$ outlet aspect ratio. These inlet and outlet channels were connected with a 180° bend. The results for smooth channel with divider wall-to-tip wall distance (W_{el}/W_{in}) = 1.5 were chosen as validation case in current study. Figure 5 shows the local Nusselt numbers at different location in the channel normalized with the Nusselt number as defined in Eq. 1. Experiments showed that the flow gets fully developed when it reaches near the bend region, so a periodic segment was used to produce the fully developed profiles which were mapped at the inlet to the computational domain shown in Fig. 1.

CFD predictions of the local Nusselt number distributions are in good agreement with the experimental results at inlet and bend bottom regions (1 and 3 respectively). At the tip wall (4), the experiments show two regions of high heat transfer separated by a lower heat transfer region. The numerical results, however predict a larger region of enhanced heat transfer due to impingement of fluid coming from inlet pass. In other words, the numerical prediction is for a shift of second heat transfer region towards the side wall at the bend region (5). At the side wall (2) in bend region the numerical prediction are very similar to the experimental results though a comparatively larger region with high heat transfer is predicted. At the side walls of the bend (5) and the outlet pass region (6), the numerical results are also comparable to the experimental results except for the bottom surface of outlet pass (6), a large recirculation region is predicted which results in reduced heat transfer close to the divider wall and increased heat transfer at the side walls possibly a result of a vena contracta in flow. But the experimental results suggest a less severe separation at the 180° bend.

The area averaged Nusselt numbers for different regions were also compared with experimental results and are shown in Table 1. At the tip wall, due to a prediction of higher impingement, the difference in numerical and experimental values is high. Though the local Nusselt number distribution at the outlet pass was different; the area average values are not that different. This means that the prediction of more abrupt change in Nusselt number has minor effect on the area average value in this case.

In the open literature, researchers have reported the computed averaged Nusselt numbers at different regions of the internal cooling channels compared it to experimental data. It has been found that RANS (Reynolds Averaged Navier–Stokes) models are known to perform somewhat worse for the flows with strong anisotropy of turbulence, for instance, in the bend area. A remedy would be to use a LES or a DES model of turbulence, which are however very time-consuming and computationally intensive making them impractical for engineering design. Su et al. [33] computed flow and heat transfer in a two-pass smooth channel (with rotation as well as non-rotation) with RANS equations in conjunction with a near-wall Reynolds stress turbulence model. The difference between the computed Nusselt numbers and experimental data at the inlet pass for non-rotating channel were found to be as high as 19% while at bend the maximum difference was found to be about 38%.

In present study the averaged Nusselt numbers at different sections of the channel are within similar accuracy to Shevchuk et al. [28], Su et al. [33], Okamura et al. [34] and Shih et al. [35]. Though at the bend it exceeds a little, the fact that the overall performance of the selected turbulence model in the inlet and outlet passes is good, and that it provided fast and robust convergence of the simulations, these advantages overweighed somewhat decreased accuracy in the bend area.

Shevchuk et al. [28], also performed numerical simulations for flow and heat transfer in the identical channel. The results were validated against experimental results by Jenkins et al. [29]. Shevchuk et al. [28] used an unstructured mesh for their numerical simulations, whereas a structured mesh has been used in the current study. A structured grid allows for more control over the mesh

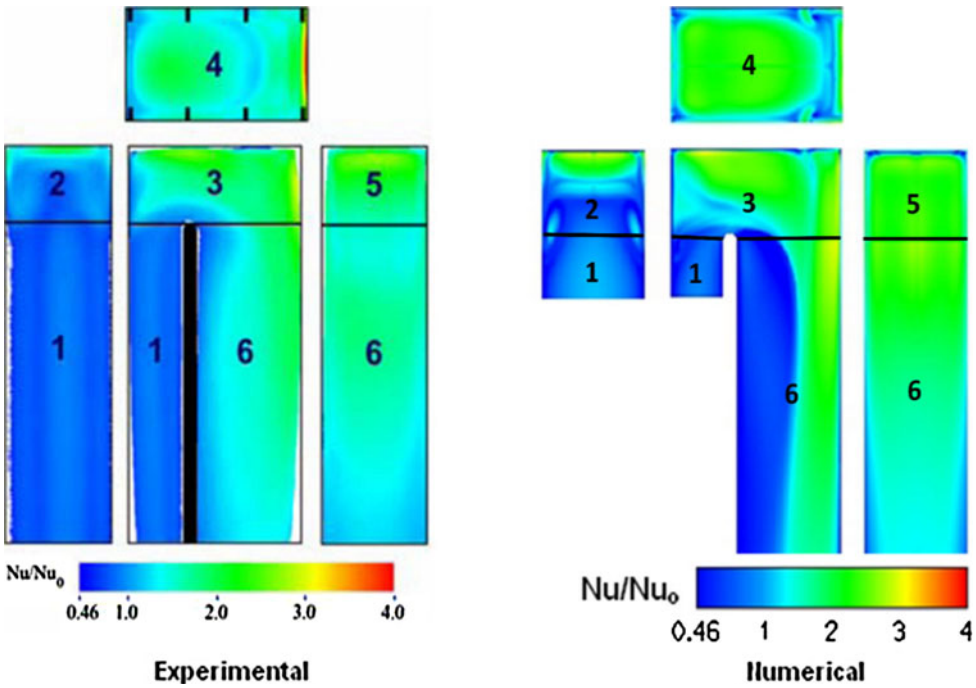

Fig. 5 Local Nusselt number distribution by experimental (*left*) and numerical (*right*) results

Table 1 Comparison of average Nusselt numbers from experiments and numerical simulation for $W_{el}/W_{in} = 1.5$

Region	Nu_{avg}/Nu_o (numerical)	Nu_{avg}/Nu_o (experimental)	Percentage difference
1 (Inlet)	0.80	0.82	2.90
2 (Bend side wall near inlet pass)	1.17	1.07	9.19
3 (Bend bottom)	1.85	1.73	6.83
4 (Tip wall)	1.91	1.59	20.30
5 (Bend side wall near outlet pass)	2.21	1.96	12.64
6 (Outlet)	1.44	1.37	4.89

parameters e.g., mesh size near the wall. Also the grid is of good quality with little cost on CPU time as it is generated faster than the unstructured mesh. The average Nusselt number for different channel sections at different tip wall-to-divider wall distances and their comparison with Shevchuk et al. [28] is shown in Fig. 6. Both simulations produced comparable results to the experiments, with maximum difference of near 8% at outlet pass for $W_{el}/W_{in} = 1$. Thus the choice of mesh type depends mainly upon the available resources and ease to handle.

4 Results and discussion

CFD simulation of a two-pass smooth channel with inlet pass aspect ratio of 1:2 has been validated against experimental results of Jenkins et al. [29] and also compared with

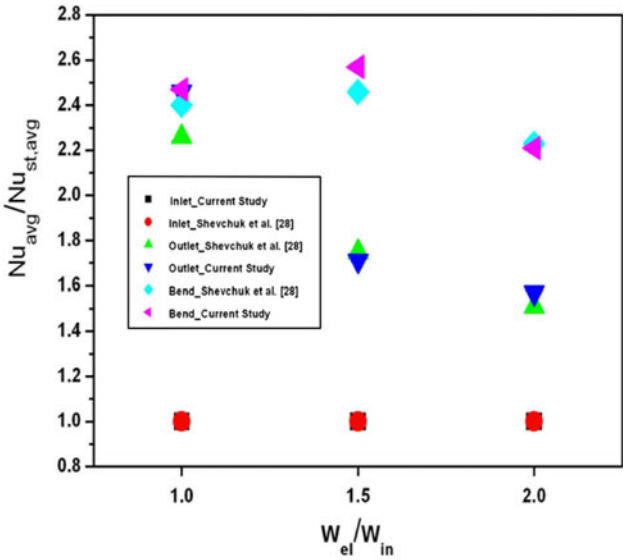

Fig. 6 Effect of W_{el} on average heat transfer in the inlet pass (faces 1a and 2), bend (face 3 and 4) and outlet pass (faces 6a and 5) as predicted in current simulation and by Shevchuk et al. [28]

CFD results of Shevchuk et al. [28]. The results, which were found satisfactory, have been presented in previous section. This numerical model is therefore accepted as bench mark to study heat transfer and flow in a two-pass smooth channel with inlet pass aspect ratio of 1:3. Prior to these studies, a smooth periodic segment was simulated. The output velocity, temperature and turbulence profiles from these segments were used as inlet to the main computational domains. Therefore, these results are discussed before presenting the main results.

4.1 Smooth periodic segment

A periodic segment of aspect ratio $W_{in}/H = 1{:}3$ was modeled and the solution for that model is used to provide inlet boundary conditions condition to the two-pass channels as well as provide a base line to study the effect of bend geometry and ribs in a two-pass channel flow.

Heat transfer enhancement as defined by Eqs. 1–3 are shown in Table 2 for $W_{in}/H = 1{:}3$. For a straight, smooth channel of aspect ratio $W_{in}/H = 1{:}2$, Shevchuk et al. [28] showed that the averages over a bottom and a side wall brought a value of $Nu_{st,avg}/Nu_o = 0.83$. While for the same geometry, experiments by Jenkins et al. [29] gave this value to be 0.82. In the current simulation, for aspect ratio $W_{in}/H = 1{:}3$, $Nu_{st,avg}/Nu_o = 0.82$.

It is also found that total averaged $Nu_{st,avg}/Nu_o$ for all walls, was equal to 0.87. Considering only the bottom wall, there is a noticeable difference between the current study for a $W_{in}/H = 1{:}3$ aspect ratio channel and a channel of aspect ratio of $W_{in}/H = 1{:}2$ by Shevchuk et al. [28]. Here the average over bottom surface predicts $Nu_{st,avg}/Nu_o = 0.62$ while in case of a channel of aspect ratio of $W_{in}/H = 1{:}2$, this vales was found to be 0.74.

Another correlation for turbulent flows in isothermal tubes by Kays et al. [31] was used to normalize the experimental results by Pape et al. [1] for a straight smooth channel of the aspect ratio $W_{in}/H = 1{:}4$. Averaging over the side and bottom surfaces gave $Nu_{st,avg}/Nu_l = 0.94$ which is also predicted in the current study. This shows that averaging over a side and bottom surface has not been affected by the aspect ratio of the channel.

A more recent correlation for turbulent flows in a channel which are influenced by isothermal wall boundaries is given by Petukhov et al. [32]. The results normalized with Petukhov's correlation are presented in Table 2, which shows that in contrast to the other two correlations, the Petukhov's correlation agrees much better with the current simulations, proving its strength in predicting the Nusselt numbers in a straight channel.

4.2 Two-pass smooth channel

Different two-pass channels with varying divider-to-tip wall distances were simulated. The results for fluid flow and heat transfer are presented separately.

4.2.1 Velocity and temperature fields

Different planes have been selected in the two-pass channel, where the fluid flow field has been obtained. Figure 7 shows these planes, which are viewed by an observer facing the duct inlet and travelling streamwise in the duct with the side walls on the left and right sides, while having the symmetry on the top.

Profiles of normalized streamwise velocity and local temperature on the symmetry plane at these streamwise positions are presented in Fig. 8. These profiles represent the case where $W_{el}/W_{in} = 1.5$.

Figure 9 shows the sequence of plots of velocity vectors, velocity magnitude contours and isotherms at these streamwise locations. This helps to give a quantitative analysis of the flow and thermal field. The inlet conditions were mapped from a periodic segment of same aspect ratio as that of the inlet pass of the two-pass channel. The flow is fully developed and the profile at the inlet in Fig. 8 is an evidence of this. Further downstream, at plane 1, the effect of pressure driven secondary flow due to the bend starts to appear and the fluid tries to follow the bend. At plane 2 (which is the center of the bend), the flow tries to be uniform, but again due to friction, it decelerates near the divider wall and this results in a big vortex at plane 2 as shown in Fig. 9. This causes high heat transfer at the tip wall of the channel. Upstream of the outlet pass (Plane 3), the fluid accelerates near left side wall. The non-uniformity of velocity results in creation of two counter rotating vortices. Xie et al. [36] has shown that for a two-pass smooth channel, where the inlet pass and outlet pass are of same aspect ratio, only one vortex remains upstream of the outlet pass.

When a fluid travels along a curved streamline path, pressure and centrifugal forces act on the fluid. These two forces balance each other in equilibrium. But in the boundary layer, due to friction, the fluid velocity decreases. This in turn results in a decrease of centrifugal forces. At the same time, the pressure forces persist. This imbalance causes a motion oriented towards the centre. As a result a long longitudinal vortex is generated near the side walls. This mechanism is referred to as the pressure-driven secondary motion. The thickness of the boundary layer dictates the strength of this motion. This motion results in moving the cold high momentum fluid from the channel

Table 2 Average Nusselt number in a smooth straight channel with $W_{in}/H = 1{:}3$ as predicted in simulations

	Bottom	Side walls	Total average	Bottom + wall
$Nu_{st,avg}$	125	192	175	165
$Nu_{st,avg}/Nu_o$	0.62	0.95	0.87	0.82
$Nu_{st,avg}/Nu_l$	0.70	1.07	0.98	0.92
$Nu_{st,avg}/Nu_{pe}$	0.73	1.13	1.03	0.97

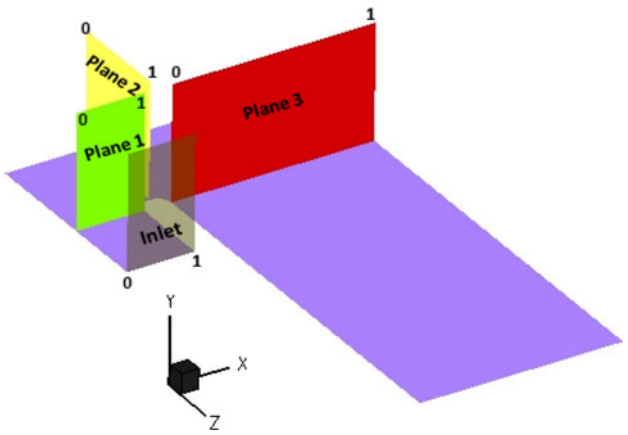

Fig. 7 Different planes in the two-pass smooth channel to plot velocity and temperature contours

core to the side walls and plays a significant role in the heat transfer phenomenon in the channel bend and outlet regions [37].

4.2.2 *Pressure drop and heat transfer*

To observe the effect of varying the divider-to-tip wall distance on pressure drop, relative pressure drop Δp^* has been calculated using Eq. (5).

$$\Delta p* = \frac{\Delta p}{0.5\rho U_{in}^2} \tag{5}$$

Figure 10 compares the relative pressure drop of the channel, as defined by Eq. 5, for an aspect ratio of inlet pass (W_{in}/H) = 1:3 with a channel having aspect ratio of 1:2 at inlet at different divider-to-tip wall distance normalized with channel inlet width (W_{in}) as well as with its height (H). For both cases the pressure drop decreases non-linearly with increasing divider-to-tip wall distance. The comparison shows that with decrease in aspect ratio, the pressure drop decreases. But as the divider-to-tip wall distance increases, this difference in pressure drop for two aspect ratio channels decreases. From $W_{el}/H = 0.4$ to 1, this difference (Δp^*) decreases from 0.4 to 0.2. For low aspect ratio case, it appears to attain a constant value after the ratio W_{el}/H reaches 0.88 or W_{el}/W_{in} reaches 2.63.

For heat transfer analysis, the channel was split into three sections as shown in Fig. 11: inlet pass (faces 1a, and 2), bend (faces1b, 3, 6b and 4) and outlet pass (faces 5 and 6a). This was done to facilitate comparison with Shevchuk et al. [28] where averaged Nusselt number was defined using volume averaged temperature of each section. Contours of $Nu_{avg}/Nu_{st,avg}$ for different cases of W_{el}/W_{in} are shown in Fig. 11. Increase in the divider-to-tip wall distance shifts, the region of enhanced heat transfer from side walls (faces 6b and 6a) and outlet pass (6), towards the section of bend region attached to the inlet pass. This accompanies a minor increase in the values of $Nu_{avg}/Nu_{st,avg}$ in the inlet. This means that with increase in W_{el}/W_{in} ratio, the flow impingement onto the outlet pass bottom (6) and external side wall (6a and 6b) weakens while the vortices get strengthened in the bend.

In order to study the effect of decrease in aspect ratio of inlet pass, the quantitative results for averaged Nusselt number at different divider-to-tip wall distances are

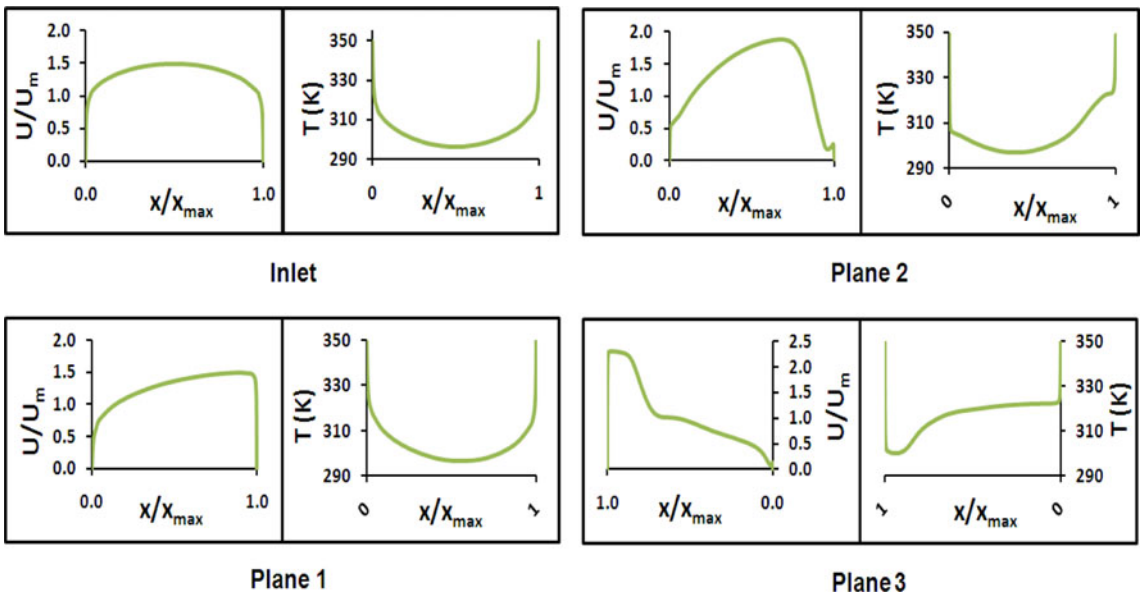

Fig. 8 Velocity and temperature profiles on the symmetry plane at different sections of the two-pass smooth channel with $W_{el}/W_{in} = 1.5$

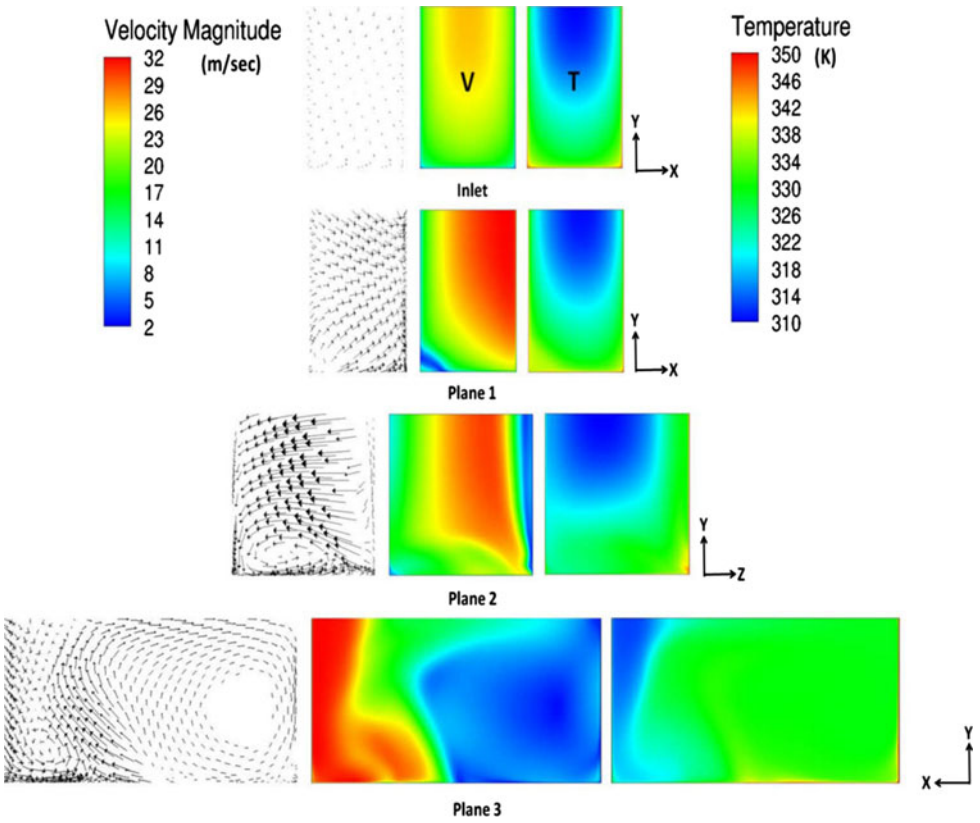

Fig. 9 Velocity field and contours of velocity magnitude and temperature (left to right) at different planes of two-pass smooth channel with $W_{el}/W_{in} = 1.5$

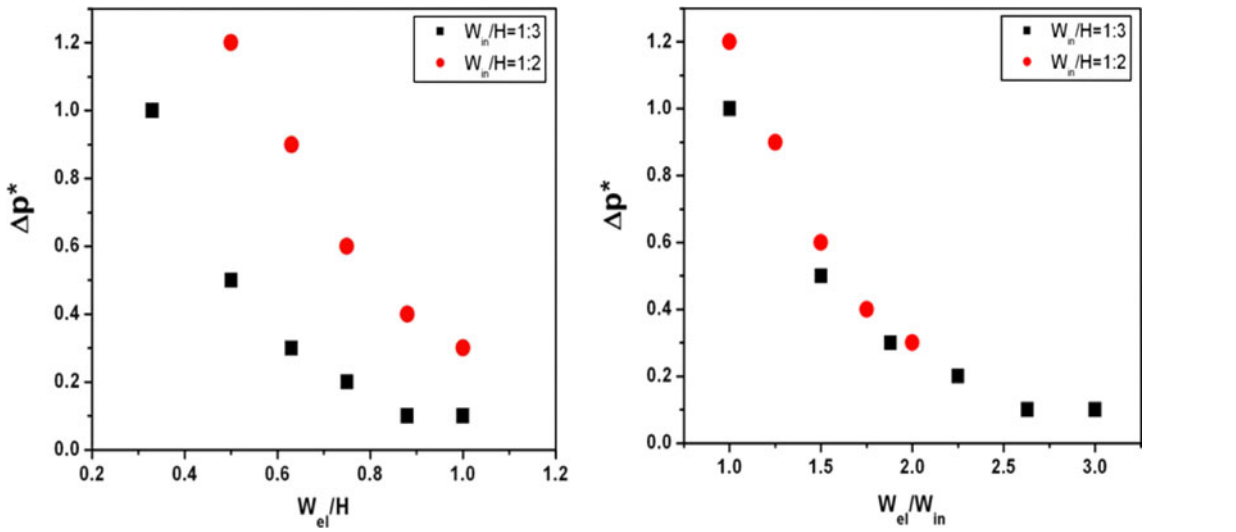

Fig. 10 Effect of W_{el} on the relative pressure drop for two-pass smooth channel

compared with the results by Shevchuk et al. [28] and is shown in Fig. 12. Again the divider-to-tip wall distance has been normalized with channel inlet width (W_{in}) as well as channel height (H). The first observation is that, with decrease in the aspect ratio from 1:2 to 1:3, heat transfer at the bend as well as at the outlet pass decreases. For a channel with inlet pass aspect ratio equal to $W_{in}/H = 1:3$, the heat transfer decreases at outlet pass with increase in W_{el}/H. Whereas in the bend, the heat transfer first decreases with increasing the gap but then increases and settles a constant value. The comparison shows that at the inlet there is a minor effect on heat transfer with decrease in aspect ratio from $W_{in}/H = 1:2$ to $W_{in}/H = 1:3$. But the trends totally differ at the bend region. For a channel with $W_{in}/H = 1:2$, heat transfer increases and then decreases with increase in

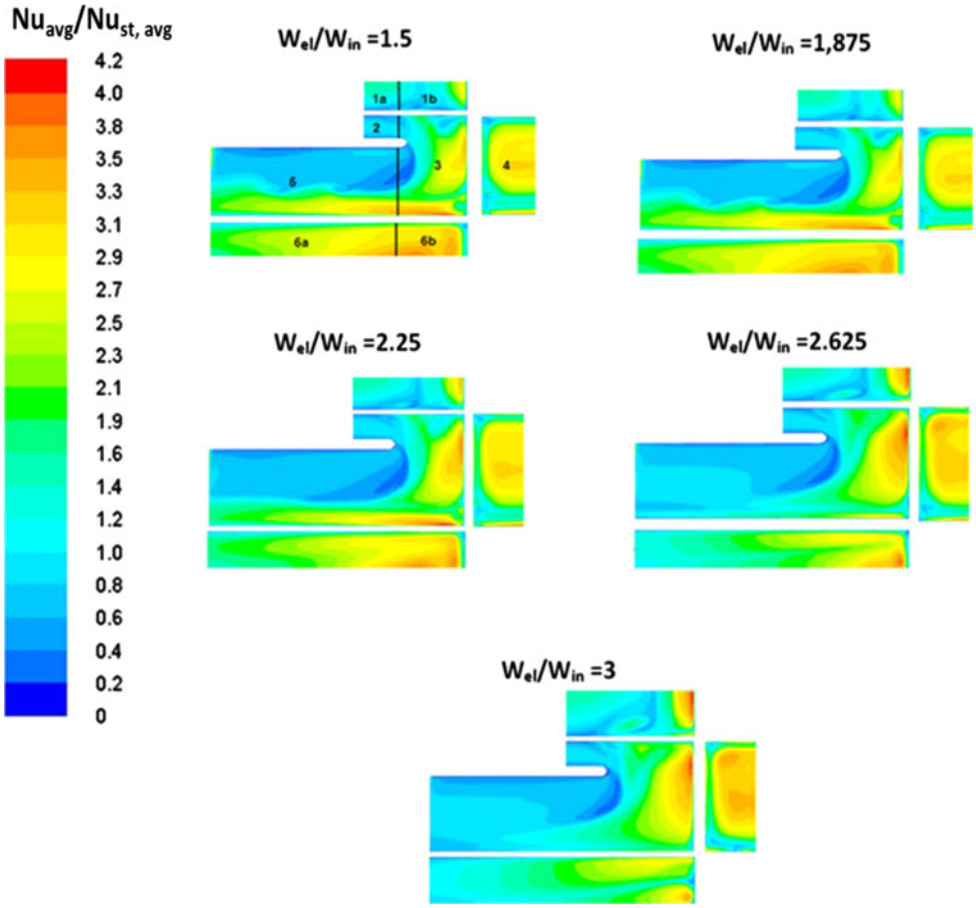

Fig. 11 Heat transfer distribution for smooth two-pass channel with aspect ratio of $W_{in}/H = 1{:}3$ and $W_{out}/H = 1{:}1$ for different W_{el}/W_{in}

W_{el}/H. In contrast, for a channel with $W_{in}/H = 1{:}3$, heat transfer decreases initially and then increases to attain a constant value independent of W_{el}/H.

To understand the reason for difference in heat transfer results for different inlet channel aspect ratio, velocity magnitudes at symmetry and near the wall are compared for a case where $W_{el}/W_{in} = 1.5$. The velocity magnitudes for both aspect ratio channels are shown in Fig. 13. The velocity magnitude for both cases is different near the wall then that at symmetry. This shows the three dimensional nature of flow. For the channel with low aspect ratio at inlet, the velocity distribution near the bottom wall is non uniform. As the divider wall-to-tip wall distance is small for the low aspect ratio channel (W_{el}/W_{in} is constant for both cases), the fluid seems to accelerate more in the bend region. This acceleration is more prominent at the symmetry plane. Due to the three dimensional nature of flow, this acceleration dies out near the wall. In contrast to that, for the high inlet aspect ratio channel, the flow becomes more uniform near the wall resulting in higher heat transfer in the bend region. At outlet pass, for low inlet aspect ratio channel, the flow accelerates more than that for high inlet aspect ratio channel. This is the reason for high heat transfer at outlet pass.

Figures 12 and 13 also show that for same W_{el}/W_{in} ratio, the channel with low inlet aspect ratio has higher heat transfer at the outlet-pass compared to the one with high inlet aspect ratio. The trend is opposite at bend region.

4.2.3 *Overall comparison*

The divider-to-tip wall distance, W_{el}, affects not only the pressure drop in the channel but also the heat transfer in bend and outlet pass of the channel. The divider-to-tip wall distance affects the heat transfer at the bottom surface of bend as well as at the tip of the channel. But it also influences the pressure drop in the channel. A parameter called thermal performance is calculated as shown in Eq. 6 which is used in the literature [38–41] to calculate the intensity of the drawback of possible pressure drop associated with the augmented heat transfer. This is used to compare the heat transfer enhancement performance at the bend region (total cumulative value for face 3 and 4).

$$\eta = \frac{Nu_{avg}/Nu_o}{(f/f_o)^{1/3}} \tag{6}$$

The results for thermal performance of bend region are presented in Fig. 14. This trend is a combined result from

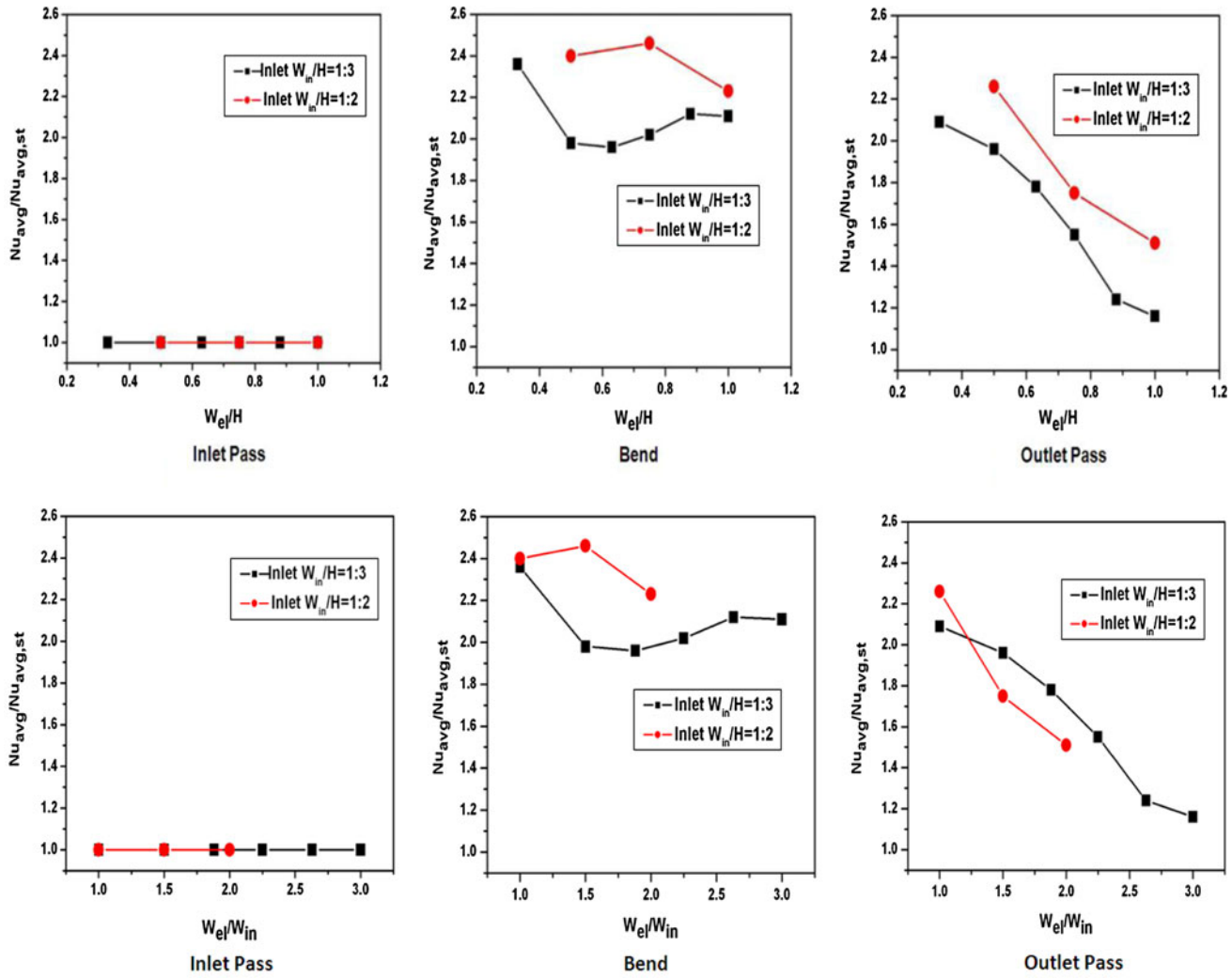

Fig. 12 Effect of the W_{el} on average heat transfer in the inlet pass (faces 1a and 2), bend (faces 3 and 4) and outlet pass (faces 6a and 5), for two channels of different inlet aspect ratios

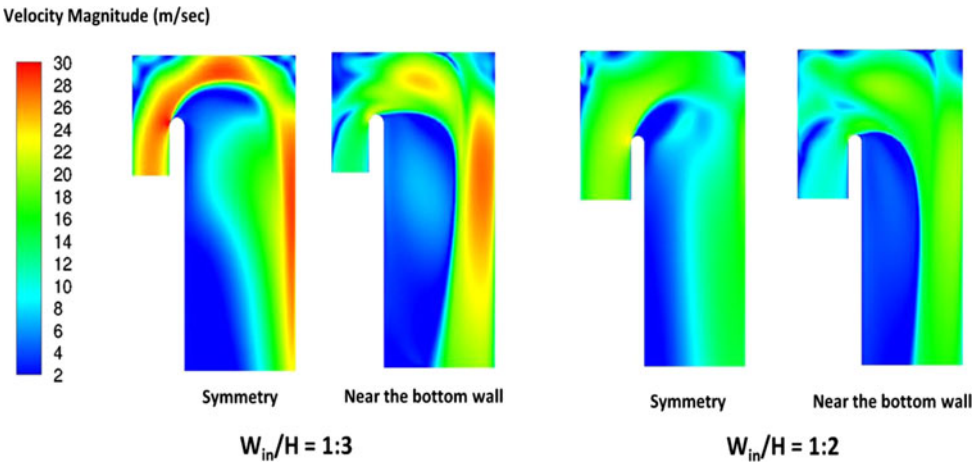

Fig. 13 Velocity magnitude distribution for two channels with $W_{el}/W_{in} = 1.5$

the trends for Δp^* (Fig. 10) and Nu_{avg}/Nu_o (Fig. 12). Pressure drop attains a constant value at $W_{el}/H = 0.88$, as shown in Fig. 10. The thermal performance at bend region continues to increase until $W_{el}/H = 0.88$, after which it tends to attain a constant value. This is the value of divider-to-tip wall distance, for a channel with inlet pass aspect

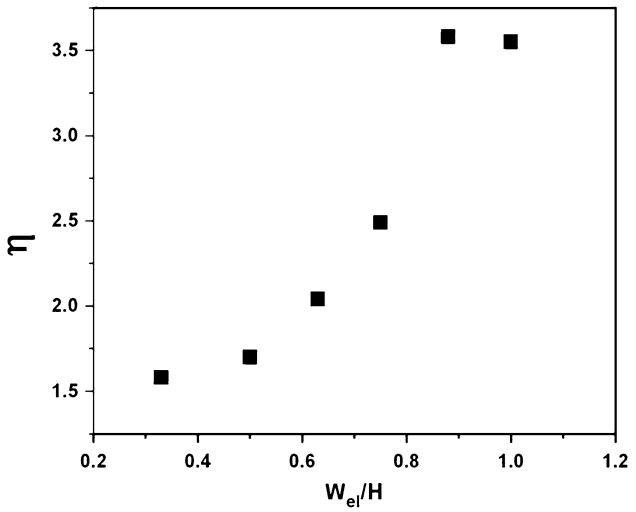

Fig. 14 Aerothermal efficiency at bend (faces 3 and 4) of the smooth two-pass channel with aspect ratio of $W_{in}/H = 1{:}3$ and $W_{out}/H = 1{:}1$ for different W_{el}/H

ratio $W_{in}/H = 1{:}3$, where maximum heat is transferred from bend region at minimum pressure drop.

5 Conclusions

The three dimensional turbulent flow and convective heat transfer in two-pass smooth channel have been numerically investigated. The inlet pass has the aspect ratio $W_{in}/H = 1{:}3$, which is connected through a 180° bend with outlet pass which has the aspect ratio $W_{out}/H = 1{:}1$. The numerical method was validated by comparing the results with the experimental results of Jenkins et al. [29] and the numerical results by Shevchuk et al. [28] which published the results for a channel with inlet pass aspect ratio equal to $W_{in}/H = 1{:}2$. The performance of the two channels with different aspect ratio inlet passes was compared. The findings are summarized as follows:

1. For convective heat transfer in a confined flow, Petukhov's correlation performs better than Dittus-Boelter's correlation in predicting the heat transfer coefficients. For a periodic channel, Petukhov's correlation improves the prediction of Nusselt number by about 15% comparing to Dittus-Boelter's correlation.
2. With an increase in W_{el}/W_{in} ratio, the relative pressure drop, Δp^*, decreases exponentially.
3. At small W_{el}/H ratio, the pressure drop decreases with increase in aspect ratio. But as this distance increases, the magnitude of difference in pressure drop for two aspect ratio channels decreases.
4. For the smooth channel, an increase in W_{el}/W_{in} ratio results in the shift of the areas of enhanced heat transfer from outlet pass to the bend region with a minor increase of heat transfer at the inlet pass.
5. There is a minor effect on heat transfer in the inlet and outlet pass of smooth channels with a decrease in the aspect ratio. For bend region, the heat transfer first decreases and then increases to attain a constant value for a low aspect ratio channel in contrast to high aspect ratio channel where it first increases and then decreases.
6. Results suggest that a high aspect ratio inlet channel (1:2) is preferable to the low aspect ratio channel (1:3) if the purpose is to enhance heat transfer at outlet-pass and the bend regions.
7. For a channel with $W_{in}/H = 1{:}3$ and $W_{out}/H = 1{:}1$, the thermal performance increases with increase in the relative tip wall distance W_{el}/H with an optimum value of 0.88.

Acknowledgments The first author acknowledges the financial support from Higher Education Commission (HEC) of Pakistan and the Division of Heat and Power, Department of Energy Technology, KTH Sweden. The support from Swedish Institute (SI) is also appreciated. The authors are thankful to Dr. Esa Utriainen from SIEMENS Industrial Turbomachinery AB, Finspång, Sweden and Professor Emeritus Torsten Strand, KTH, Stockholm Sweden for valuable discussions. This work was supported by grants of computer time from Parallel Computer Center (PDC) at KTH, Stockholm, Sweden.

References

1. Pape D, Jeanmart H, von Wolfersdorf J, Weigand B (2004) Influence of the 180° bend geometry on the pressure loss and heat transfer in a high aspect ratio rectangular smooth channel. Proceedings of the 2004 ASME Turbo Expo (June 14-17, 2008, Vienna, Austria), GT2004-53753
2. Mochizuki S, Murata A, Shibata R, Wen-Jei Yang (1998) Detailed measurements of local heat transfer coefficients in turbulent flow through smooth and rib-roughened serpentine passages with a 180 sharp bend. Intl J Heat Mass Transfer 42(11):1925–1934
3. Hirota M, Fujita H, Syuhada A, Araki S, Yoshida T, Tanaka T (1999) Heat/mass transfer characteristics in two-pass smooth channels with a sharp 180-deg turn. Int J Heat Mass Transfer 42(20):3757–3770
4. Hirota M, Fujita H, Cai L, Nakayama H, Yanagida M, Syafa'at A (2002) Heat (mass) transfer in rectangular cross-sectioned two-pass channels with an inclined divider wall. Int J Heat Mass Transfer 45(5):1093–1107
5. Cai L, Ota H, Hirota M, Nakayama H, Fujita H (2004) Influence of channel aspect ratio on heat transfer characteristics in sharp-turn connected two-pass channels with inclined divider wall. Exp Thermal Fluid Sci 28(6):513–523
6. Mockizuki S, Murata A, Shivata R, Yang WJ (1999) Detailed measurements of local heat transfer coefficients in turbulent flow through smooth and rib-roughened serpentine passages with a 180 sharp bend. Int. J Heat Mass Transfer 42:1925–1934
7. Cho HH, Lee SY, Rhee DH (2004) Effects of cross ribs on heat/mass transfer in a two-pass rotating duct. Heat and Mass Transfer 40:743–755

8. Schüler M, Dreher HM, Neumann SO, Weigand B (2010) Numerical predictions of the effect of rotation on fluid flow and heat transfer in an engine-similar two-pass internal cooling channel with smooth and ribbed walls. Proceedings of ASME Turbo Expo 2010, GT2010-22870
9. Xie G, Sundén B, Wang L, Utriainen E (2011) Parametric study on heat transfer enhancement and pressure drop of an internal blade tip-wall with pin-fin arrays. Heat Mass Transfer 47:45–57
10. Schabacker J, Boelcs A, Johnson V (1998) PIV investigation of the flow characteristics in an internal coolant passage with two ducts connected by a sharp 180° bend. Proceedings of the 1998 ASME Turbo Expo, GT-544
11. Liou TM, Chen CC (1999) Heat transfer in a rotating two-pass smooth passage with a 180 rectangular turn. Int J Heat Mass Transfer 42:231–247
12. Chen CC, Liou TM (2000) Rotating effect on fluid flow in a smooth duct with a 180-deg sharp turn. Proceedings of the 2000 ASME Turbo Expo, GT-0228
13. Son SY, Kihm KD, Han JC (2002) PIV flow measurements for heat transfer characterization in two-pass square channels with smooth and 90 ribbed walls. Int J Heat Mass Transfer 45:4809–4822
14. Elfert M, Jarius MP, Weigand B (2004) Detailed flow investigation using PIV in a typical turbine cooling geometry with ribbed walls. Proceedings of the 2004 ASME Turbo Expo, GT2004-53566
15. Park CW, Lau SC (1998) Effect of channel orientation of local heat (mass) distributions in a rotating two-pass square channel with smooth walls. ASME J Heat Transfer 120:624–632
16. Han JC, Chandra PR, Lau SC (1988) Local heat/mass transfer distributions around sharp 180 deg turns in two-pass smooth and rib- roughened channels. ASME J Heat Transfer 110:91–98
17. Wang T, Chyu MK (1994) Heat convection in a 180-deg turning duct with different turn configurations. J Thermophysics Heat Transfer 8(3):595–601
18. Liou TM, Chen CC, Chen MY (2003) Rotating Effect on fluid Flow in Two Smooth Ducts Connected by a 180° Bend. J. Fluid Engineering 125:138–148
19. Etemad S, Sundén B (2006) Numerical investigation of turbulent heat transfer in a rectangular-sectioned 90° bend. Numer Heat Transfer A 49:323–343
20. Salameh T, Sundén B (2010) An experimental study of heat transfer and pressure drop on the bend surface of a U-duct. Proceedings of the 2010 ASME Turbo Expo, GT2010-22139
21. Han JC (1988) Heat transfer and friction characteristics in rectangular channels with rib turbulators. ASME J Heat Transfer 110:321–328
22. Han JC, Park JS (1988) Developing heat transfer in rectangular channels with rib turbulators. Int J Heat and Mass Transfer 31:183–195
23. Park JS, Han JC, Huang Y, OU S (1992) Heat transfer performance comparison of five different rectangular channels with parallel angled ribs. Int J Heat and Mass Transfer 35(11):2891–2903
24. Astarita T, Cardone G (2000) Thermofluidynamic analysis of the flow in a sharp 180 deg turn channel. Exp Thermal and Fluid Science 20:118–200
25. Cai L, Ota H, Hirota M, Nakayama H, Fujita H (2004) Influence of channel aspect ratio on heat transfer characteristics in sharp-turn connected two-pass channels with inclined divider wall. Exp Thermal and Fluid Science 28:513–523
26. Siddique W, El-Gabry L, Shevchuk IV, Fransson T (2011) Validation and analysis of numerical results for a two-pass trapezoidal channel with different cooling configurations of trailing edge. Proceedings of the 2011 ASME Turbo Expo, GT2011-46266
27. ANSYS FLUENT User's Guide (2009) Version 12, ANSYS Inc
28. Shevchuk IV, Jenkins SC, Weigand B, von Wolfersdorf J, Neumann SO, Schnieder M (2011) Validation and analysis of numerical results for a varying aspect ratio two-pas internal cooling channel. ASME J Heat Transfer 133(5):051701
29. Jenkins SC, Zehnder F, Shevchuk IV, von Wolfersdorf J, Weigand B (2008) The effect of ribs and tip wall distance on heat transfer for a varying aspect ratio two-pass ribbed internal cooling channel. Proceedings of the 2008 ASME Turbo Expo (June 9–13, 2008, Berlin, Germany), vol 4, Pts. A and B, pp 1051–1061
30. Incropera FP, de Witt DP (2002) Fundamentals of heat and mass transfer, 5th edn. Wiley, New York
31. Kays WM, Crawford ME, Weigand B (2005) Convective heat and mass transfer, 4th edn. Mc Graw-Hill, New York
32. Petukhov BS, Irvine TF, Hartnett JP (1970) Advances in heat transfer, vol 6. Academic Press, New York
33. Su G, Chen HC, Han JC, Heidmann JD (2004) Computation of flow and heat transfer in rotating two-pass rectangular channels (AR = 1:1, 1:2, and 1:4) with smooth walls by a Reynolds stress turbulence model. Int J Heat and Mass Transfer 47(26):5665–5683
34. Okamura T, Koga A, Kawagishi H (2002) Heat transfer in high-aspect-ratio rectangular passage with skewed ribs. Heat Transfer-Asian Research 31(2):89–104
35. Shih TI, Lin YL, Stephens MA (2001) Fluid flow and heat transfer in an internal coolant passage. Int J Rotating Machinery 7(5):351–364
36. Xie GN, Sundén B, Wang L, Utriainen E (2009) Augmented heat transfer of an internal blade tip wall with pin-fins. Proceedings of the 2009 ASME Turbo Expo (June 8–12, 2008, Orlando, Florida, USA), GT2009–59410
37. Etemad S (2005) Computational analysis of heat transfer and fluid flow with relevance for IC-engine cooling. Dissertation, Lund Institute of Technology, Lund, Sweden
38. Gee DL, Webb RL (1980) Forced convection heat transfer in helically rib-roughened tubes. Int J Heat and Mass Transfer 23:1127–1136
39. Han JC, Park JS, Lei CK (1985) Heat transfer enhancement in channels with turbulence promoters. J Eng Gas Turbines Power 107:628–635
40. Bonhoff B, Parneix S, Leusch J, Johnson BV, Schabacker J, Bölcs A (1999) Experimental and numerical study of developed flow and heat transfer in coolant channels with 45° ribs. Int J Heat and Fluid Flow 20:311–319
41. Salameh T, Sundén B (2011) Effects of ribs on internal blade-tip cooling. Proceedings of the 2011 ASME Turbo Expo (Vancouver, Canada) GT2011–45118